An Improved Discontinuous Space Vector Modulation Scheme for the Three-Phase Impedance Source Inverters

Ahmed Abdelhakim*, Frede Blaabjerg†, Paolo Mattavelli*
*Dept. of Management and Engineering, University of Padova, Vicenza, Italy
†Dept. of Energy Technology, Aalborg University, Aalborg, Denmark
Email: ahmed.a.abdelrazek@ieee.org, fbl@et.aau.dk, paolo.mattavelli@unipd.it

***Abstract*—Among various modulation schemes that can be used with the three-phase impedance source inverters, discontinuous modulation schemes are seen to be worthwhile due to the resultant reduction in the switching losses. Depending on the employed method of achieving the shoot-through (ST) state, these discontinuous modulation schemes can be classified into two categories: three-phase-leg ST-based (3P) and single-phase-leg ST-based (1P) discontinuous modulation schemes. This paper considers the 1P maximum boost discontinuous space vector modulation (1P/MB/DSVM) scheme and improves it in terms of simplifying the gate signals generation and increasing the conversion efficiency for the same operating conditions. In this paper, the conventional and the improved 1P/MB/DSVM schemes are analyzed and compared, where the analysis and comparison are enhanced with simulation results using PLECS. Finally, a three-phase quasi-Z-source inverter (qZSI) prototype is utilized to verify the reported analysis and simulation results, demonstrating an improved conversion efficiency using the improved 1P/MB/DSVM scheme.**

***Index Terms*—Discontinuous modulation, impedance source inverter, pulse width modulation (PWM), quasi-Z-source inverter (qZSI), renewable energy, space vector modulation (SVM), Z-source inverter (ZSI).**

I. Introduction

The diffusion of the renewable energy sources (RESs) into the power system is continuously increasing, which stimulates a continuous improvement in the employed power conditioning stage (PCS) in terms of the used structures, their modulation, and control schemes [1]–[4]. Among the possible PCSs, the boost converter-fed voltage source inverter (VSI) PCS, which is commonly called two-stage PCS, is mandatory for some applications, such as photovoltaic (PV) and fuel cell, due to their low and/or non-regulated output dc voltage [5]. On the other hand, single-stage PCSs, represented in the impedance source inverters, introduce an interesting alternative to this two-stage architecture [6]–[10].

These impedance source inverters are gaining high attention due to two fundamental reasons. The first reason is the embracement of the boosting capability within the inversion operation, i.e. they can work as buck-boost inverters. The second reason is the utilization of an additional switching state, called shoot-through (ST) state, which prevents the mandatory need of the dead-time generation. It is worth to note that the ST state is permissible in this family of power inverters due to the utilization of an impedance network between the dc source and the inverter bridge as shown in Fig. 1 for the three-phase quasi-Z-source inverter (qZSI) [6], [11]. Note that the qZSI structure shown in Fig. 1 is used in the rest of this paper as it is the commonly used impedance source inverter due to its simple structure and continuous input current compared to the other structures [8], [12].

Many various modulation schemes can be used in order to modulate the three-phase impedance source inverters [13]–[16]. These schemes can be classified into the following two categories depending on the employed method of achieving the ST state:

- three-phase-leg ST-based (3P) modulation schemes, in which the ST state is achieved using the three phase-legs simultaneously;
- single-phase-leg ST-based (1P) modulation schemes, in which the ST state is achieved using one phase-leg at a time.

Furthermore, both categories embrace continuous and discontinuous modulation schemes, where the latter modulation scheme is seen to be worthwhile due to the resultant reduction in the switching losses [14].

This paper is concerned with the 1P discontinuous modulation schemes with maximum boost (MB) capability [14]–[16], where an improved 1P/MB discontinuous space vector modulation (1P/MB/DSVM) scheme is proposed. Compared to the conventional 1P/MB/DSVM scheme, the improved one has the following merits:

- simpler generation of the gate signals, i.e. reduced implementation complexity;
- the switches are commutating at the ST current for shorter period during the fundamental period;
- reduced switching losses and improved conversion efficiency.

The rest of this paper is organized as follows: Section II reviews the operation of the three-phase qZSI and discusses its modulation using the conventional 1P/MB/DSVM scheme. Then, Section III introduces the improved 1P/MB/DSVM scheme and compares it with the conventional one. In order to verify the prior reported analysis, Section IV introduces the obtained simulation results, including the calculated

978-1-5386-1180-7/18/$31.00 ©2018 IEEE

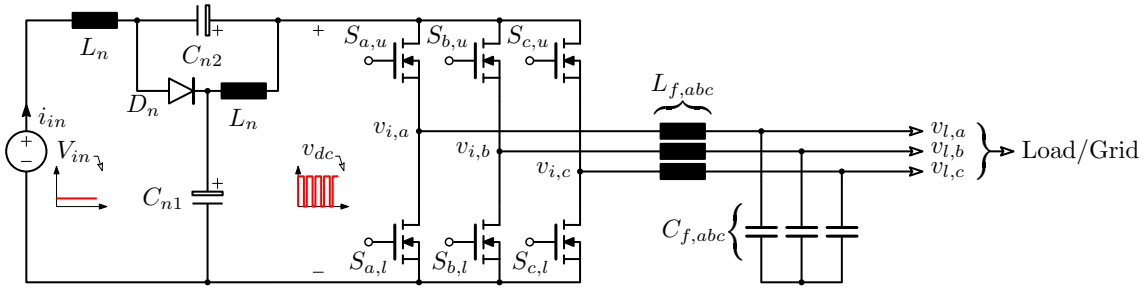

Fig. 1. Circuit diagram of the three-phase quasi-Z-source inverter (qZSI) with an output LC filter.

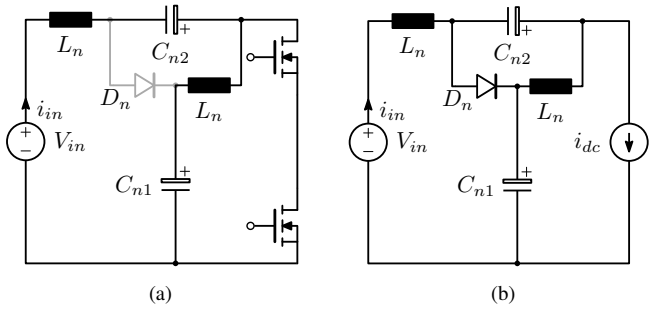

Fig. 2. Equivalent circuits of the qZSI during the ST and the non-ST states. (a) During the ST state and the B6-bridge becomes equivalent to a short circuit; and (b) during the non-ST states and the B6-bridge becomes equivalent to a current source.

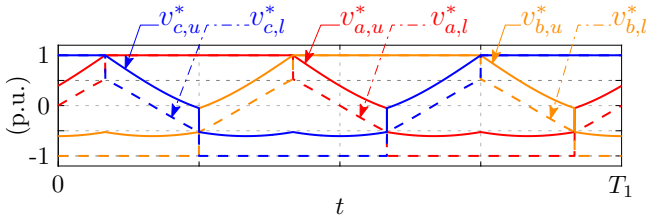

Fig. 3. Reference signals of the conventional single-phase-leg ST-based maximum boost discontinuous space vector modulation (1P/MB/DSVM) scheme, where the modulation index (M) is equal to 0.7 and T_1 is the fundamental period. Note that for any phase-leg x, $v_{x,u}$ is used to modulate $S_{x,u}$, while $v_{x,l}$ is used to modulate $S_{x,l}$.

switching losses, for both the conventional and the improved 1P/MB/DSVM schemes using PLECS. Moreover, the obtained experimental results utilizing a three-phase qZSI prototype are presented in Section V, which verify the functionality of the improved 1P/MB/DSVM scheme and demonstrate an improved conversion efficiency. Finally, conclusions are drawn in Section VI.

II. Review of the Three-Phase qZSI Operation and Modulation

A. Operation of the Three-Phase qZSI

The three-phase qZSI shown in Fig. 1 inserts an impedance network, which comprises two identical inductors ($2L_n$), two capacitors (C_{n1} and C_{n2}), and a diode (D_n), between the input dc source (V_{in}) and the employed B6-bridge [8]. This impedance network allows the use of an additional switching state, called ST state, under which the B6-bridge becomes equivalent to a short circuit as shown in Fig. 2(a). On the other hand, this B6-bridge is equivalent to a current source during the non-ST states as shown in Fig. 2(b).

Such utilization of the ST state results in a discontinuous dc-link voltage (v_{dc}), which is pulsating between zero and a peak value of $\hat{v}_{dc}$ for a continuous conduction mode of operation. Note that $\hat{v}_{dc}$ is controlled by controlling the ST state equivalent time. Moreover, this ST state must be inserted inside the zero states, i.e. all or part of the conventional zero states equivalent time is assigned to the ST state, in order not to affect the active states and the output voltage.

B. Modulation of the Three-Phase qZSI

Under any modulation scheme, the qZSI shown in Fig. 1 is modulated in order to obtain a three-phase symmetrical output voltage, where the output fundamental peak phase voltage given by

$$\hat{V}_{\varphi 1} = M \cdot \frac{\hat{v}_{dc}}{2}, \tag{1}$$

where M is the modulation index and $\hat{v}_{dc}$ is the peak dc-link voltage given by

$$\hat{v}_{dc} = \frac{V_{in}}{1 - 2D_{ST}}, \tag{2}$$

being V_{in} is the input dc voltage and D_{ST} is the average of the ST duty cycle (d_{ST}), which differs from one modulation scheme to another one.

As mentioned before, the qZSI can be modulated using many various modulation schemes, where this paper is concerned with the conventional 1P/MB/DSVM scheme, whose reference signals are shown in Fig. 3. According to [14], [16], these reference signals are given by

$$\begin{aligned} v^*_{max,u} &= v^*_{max} \\ v^*_{max,l} &= v^*_{max}, \end{aligned} \tag{3}$$

$$\begin{aligned} v^*_{mid,u} &= v^*_{mid}, \\ v^*_{mid,l} &= v^*_{mid} - d_{ST}, \end{aligned} \tag{4}$$

$$\begin{aligned} v^*_{min,u} &= v^*_{min} - d_{ST}, \\ v^*_{min,l} &= v^*_{min} - 2d_{ST}, \end{aligned} \tag{5}$$

where

$$\begin{aligned} v^*_{max} &= max(v^*_a, v^*_b, v^*_c), \\ v^*_{mid} &= mid(v^*_a, v^*_b, v^*_c), \\ v^*_{min} &= min(v^*_a, v^*_b, v^*_c), \end{aligned} \tag{6}$$

$$\begin{aligned} v^*_{max,u} &= max(v^*_{a,u}, v^*_{b,u}, v^*_{c,u}), \\ v^*_{max,l} &= max(v^*_{a,l}, v^*_{b,l}, v^*_{c,l}), \end{aligned} \tag{7}$$

$$\begin{aligned} v^*_{mid,u} &= mid(v^*_{a,u}, v^*_{b,u}, v^*_{c,u}), \\ v^*_{mid,l} &= mid(v^*_{a,l}, v^*_{b,l}, v^*_{c,l}), \end{aligned} \tag{8}$$

$$\begin{aligned} v^*_{min,u} &= min(v^*_{a,u}, v^*_{b,u}, v^*_{c,u}), \\ v^*_{min,l} &= min(v^*_{a,l}, v^*_{b,l}, v^*_{c,l}), \end{aligned} \tag{9}$$

being v^*_a, v^*_b, and v^*_c are given by

$$\begin{aligned} v^*_a &= 1, \\ v^*_b &= 1 - M \cdot \{\frac{3}{2} sin(\omega_1 t) - \frac{\sqrt{3}}{2} cos(\omega_1 t)\}, \\ v^*_c &= 1 - M \cdot \{\frac{3}{2} sin(\omega_1 t) + \frac{\sqrt{3}}{2} cos(\omega_1 t)\}, \end{aligned} \tag{10}$$

where $\frac{\pi}{6} \leq \omega_1 t \leq \frac{5\pi}{6}$ and ω_1 is the fundamental angular frequency, which is equal to $2\pi f_1$, while f_1 is the fundamental frequency.

Finally, the ST duty cycle (d_{ST}) is variable during the fundamental period and it is given by

$$d_{ST} = 1 - \frac{\sqrt{3}M}{2} sin(\omega_1 t + \frac{\pi}{6}), \tag{11}$$

where $\frac{\pi}{6} \leq \omega_1 t \leq \frac{\pi}{2}$, and its average (i.e. D_{ST}) is given by

$$D_{ST} = 1 - \frac{3\sqrt{3}M}{2\pi}. \tag{12}$$

Under this conventional 1P/MB/DSVM scheme, each switch in the B6-bridge has its equivalent reference signal. For example, $S_{a,u}$ is turned ON when $v^*_{a,u}$ is larger than the carrier signal and turned OFF when this condition is not true, while $S_{a,l}$ is turned ON when $v^*_{a,l}$ is smaller than the carrier signal and turned OFF when this condition is not true. Note that the ST state is inserted by overlapping each two switches in the same phase-leg during their commutation instants.

III. Improved 1P/MB/DSVM Scheme

From the prior discussions, it can be seen that the conventional 1P/MB/DSVM scheme, shown in Fig 3, suffers from the following demerits:

- complicated generation of the gate signals due to the complicated calculation of the reference signals;
- although the ST state is inserted three times during each switching cycle, the effective switching frequency of the impedance network is varying from one to three times the carrier frequency due to the variation of the active states equivalent time. Thus, the impedance network must be designed based on the lowest value of the effective switching frequency which is equal to the carrier frequency;
- the lower switches are commutating at the ST current for one-third of the fundamental period, while the upper switches are commutating at the ST current for two-third of the fundamental period.

Hence, this paper proposes an improved 1P/MB/DSVM scheme in order to overcome these demerits, where this improved modulation scheme is depicted in Fig. 4.

A. Principle of Operation

Unlike the conventional 1P/MB/DSVM scheme which is shown in Fig 3, the improved 1P/MB/DSVM scheme uses three reference signals as shown in Fig. 4. Note that these reference signals are commonly used with the traditional three-phase VSIs, and they are given by (10).

Using this improved 1P/MB/DSVM scheme, the three-phase qZSI is modulated as follows: for any phase-leg x, $S_{x,u}$ is turned ON when v^*_x is larger than the carrier signal, while $S_{x,l}$ is turned ON when v^*_x is smaller than the carrier signal or is the smallest reference signal as shown in Fig. 4. In this way, the ST is achieved via phase-leg x when v^*_x is the smallest reference signal. For example, $S_{a,u}$ is turned ON when v^*_a is larger than the carrier signal, while $S_{a,l}$ is turned ON when v^*_a is smaller than the carrier signal or is smaller than v^*_b and v^*_c.

As a consequence of using the improved 1P/MB/DSVM scheme, the upper switches are commutating at the ST current for one-third of the fundamental period, while the lower switches never commutate at the ST current. Furthermore, the effective switching frequency of the impedance network is fixed at the carrier frequency. On the other hand, the improved modulation scheme has the same variable ST duty cycle (d_{ST}) of the conventional one, where d_{ST} and its average (D_{ST}) are given by (11) and (12). Hence, $\hat{V}_{\varphi 1}$ is related to V_{in} using the same prior equations of the conventional 1P/MB/DSVM scheme, i.e. using (1) and (2).

In order to properly design the impedance network under the improved 1P/MB/DSVM scheme, the same procedure followed in [8] can be utilized here. Hence, the required inductance and capacitance can be estimated, considering both the low and the high frequency components, from

$$\begin{aligned} L_n \approx & \frac{\sqrt{3}M \cdot V_{in}}{70\pi(3\sqrt{3}M - \pi) \cdot f_1 \cdot \Delta I_L} \\ & + \frac{3\sqrt{3}M \cdot (\pi - 3\sqrt{3}M) \cdot V_{in}}{4(3\pi\sqrt{3}M - \pi^2) \cdot f_s \cdot \Delta I_L}, \end{aligned} \tag{13}$$

$$\begin{aligned} C_{n1} &\approx \frac{\sqrt{3}M \cdot I_{in}}{35\pi^2 \cdot f_1 \cdot \Delta V_{C_{n1}}} + \frac{(2\pi - 3\sqrt{3}M) \cdot I_{in}}{2\pi f_s \cdot \Delta V_{C_{n1}}}, \\ C_{n2} &\approx \frac{\sqrt{3}M \cdot I_{in}}{35\pi^2 \cdot f_1 \cdot \Delta V_{C_{n2}}} + \frac{(2\pi - 3\sqrt{3}M) \cdot I_{in}}{2\pi f_s \cdot \Delta V_{C_{n2}}}, \end{aligned} \tag{14}$$

where f_s is the switching frequency, I_{in} is the average input dc current, ΔI_L is the peak-to-peak inductor current ripple, and $\Delta V_{C_{n1}}$ and $\Delta V_{C_{n2}}$ are the peak-to-peak capacitor voltage ripples across C_{n1} and C_{n2} respectively. Note that these

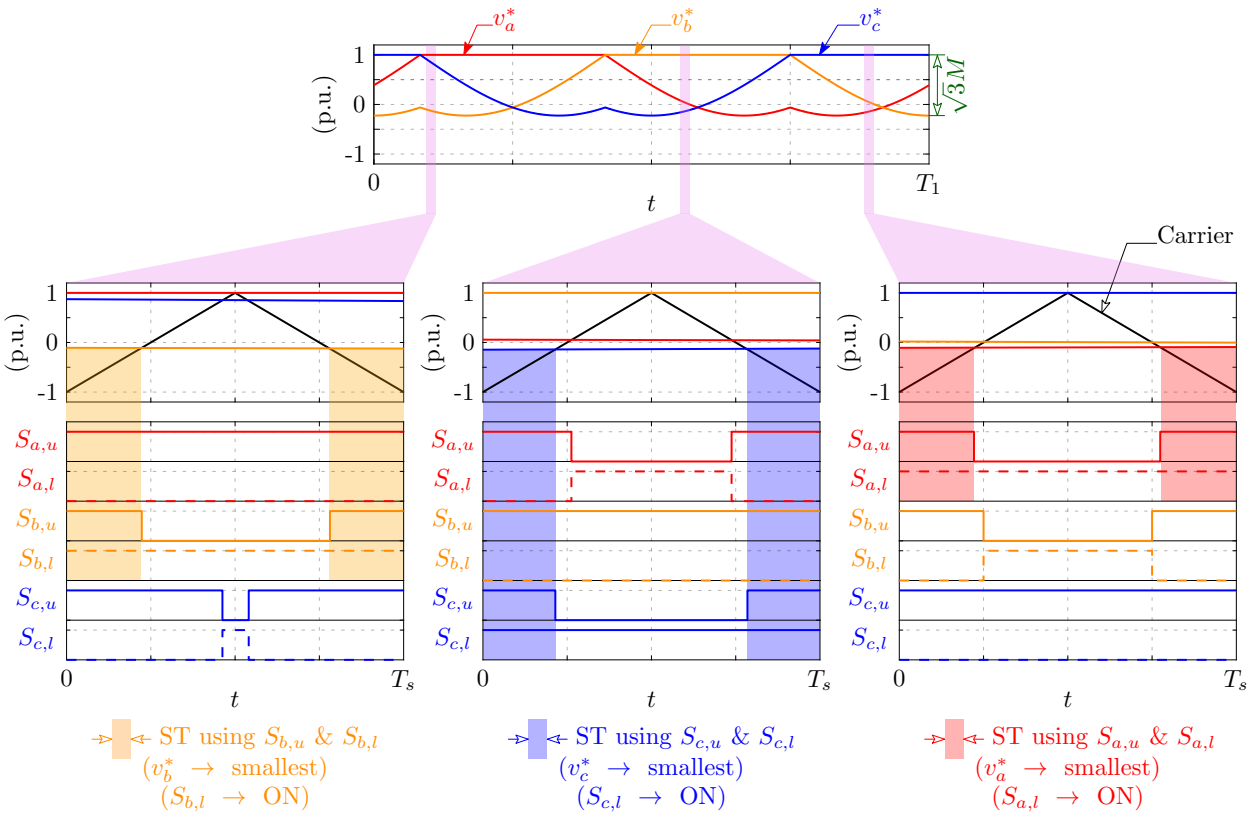

Fig. 4. Reference, carrier, and gate signals of the improved 1P/MB/DSVM scheme, where $M = 0.7$. Note that $S_{a,l}$ is maintained ON when v_a^* is the smallest reference signal, $S_{b,l}$ is maintained ON when v_b^* is the smallest reference signal, while $S_{c,l}$ is maintained ON when v_c^* is the smallest reference signal.

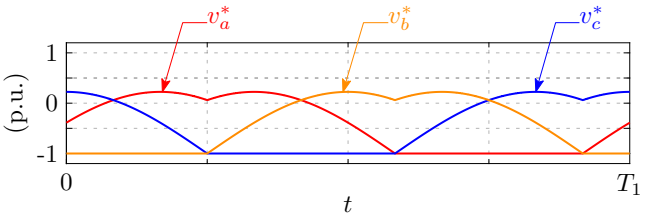

Fig. 5. Reference signals of the improved 1P/MB/DSVM scheme with negative dc clamping.

equations are also used in order to design the impedance network under the conventional 1P/MB/DSVM scheme.

It is worth to note that the improved 1P/MB/DSVM scheme is conceptually similar to the modulation scheme proposed in [11]. Meanwhile, the latter one, i.e. the modulation scheme proposed in [11], is not a discontinuous one.

Finally, note that the DSVM scheme can be achieved with positive dc clamping which is utilized in this paper, or with negative dc clamping which is similar to the positive dc clamping [14]. This can be clarified by considering the reference signals of the improved 1P/MB/DSVM scheme with negative dc clamping that is shown in Fig. 5, under which the three-phase qZSI is modulated as follows: for any phase-leg x, $S_{x,u}$ is turned ON when v_x^* is larger than the carrier signal or is the largest reference signal, while $S_{x,l}$ is turned ON when

TABLE I
COMPARISON BETWEEN THE CONVENTIONAL AND THE IMPROVED 1P/MB/DSVM SCHEMES

	Conventional	Improved
Ref. signals	Fig. 3	Fig. 4
Num. of ref. signals	6	3
Complexity	High	Low
ST duty cycle (d_{ST}) variation	Yes	
Average ST duty cycle (D_{ST})	$1-\frac{3\sqrt{3}M}{2\pi}$	
Normalized peak dc-link voltage ($\hat{v}_{dc}/V_{in}$)	$\frac{\pi}{3\sqrt{3}M-\pi}$	
Normalized output peak phase voltage ($\hat{V}_{\varphi 1}/V_{in}$)	$\frac{\pi M}{6\sqrt{3}M-2\pi}$	
$S_{abc,u}$ normalized ST duration ($T_{ST,u}/T_1$)	$\frac{2}{3}$	$\frac{1}{3}$
$S_{abc,l}$ normalized ST duration ($T_{ST,l}/T_1$)	$\frac{1}{3}$	0

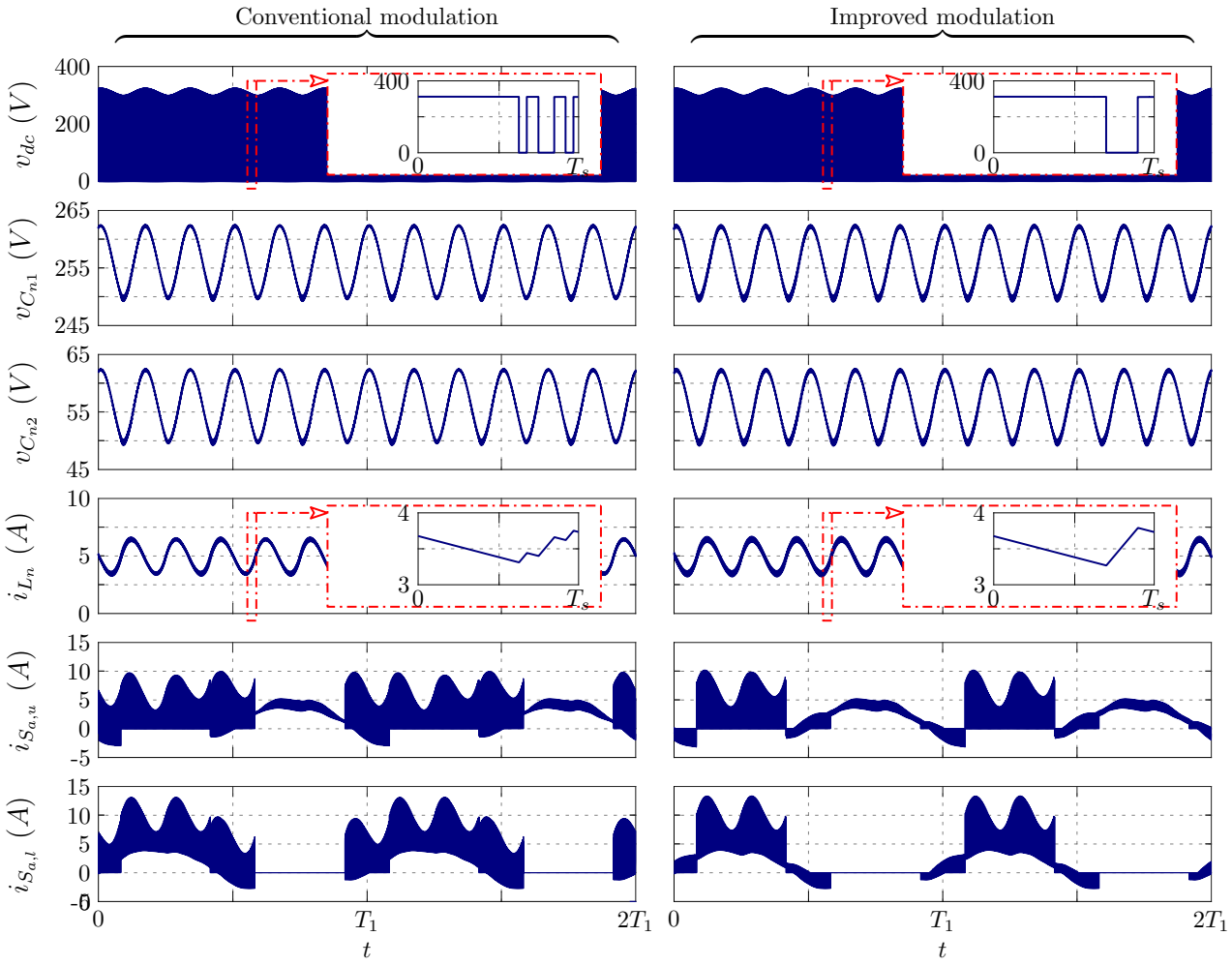

Fig. 6. Simulation results of the *1 kVA* qZSI using the conventional and the improved 1P/MB/DSVM schemes. For each modulation scheme, the dc-link voltage (v_{dc}), impedance network capacitors voltages ($v_{C_{n1}}$ and $v_{C_{n2}}$), impedance network inductor current (i_{L_n}), and upper and lower switches currents of phase a ($i_{S_{a,u}}$ and $i_{S_{a,l}}$) are shown from top to bottom.

TABLE II
PARAMETERS OF THE USED *1 kVA* THREE-PHASE QZSI

V_{in}	200 V	V_{φ_1}	110 V (RMS)	M	0.8564
f_s	60 kHz	L_n	1.6 mH	$C_{n1,2}$	20 μF
f_1	200 Hz	$L_{f,abc}$	0.35 mH	$C_{f,abc}$	4.7 μF

v_x^* is smaller than the carrier signal.

B. Comparative Study

In order to highlight and summarize the entire differences between the conventional and the improved 1P/MB/DSVM schemes, Table I compares both schemes from several aspects. These aspects include number of reference signals, implementation complexity, ST duty cycle (d_{ST}) variation, average ST duty cycle (D_{ST}), normalized peak dc-link voltage ($\hat{v}_{dc}/V_{in}$), normalized output fundamental peak phase voltage ($\hat{V}_{\varphi 1}/V_{in}$), normalized ST duration for the upper switches ($T_{ST,u}/T_1$), and normalized ST duration for the lower switches ($T_{ST,l}/T_1$).

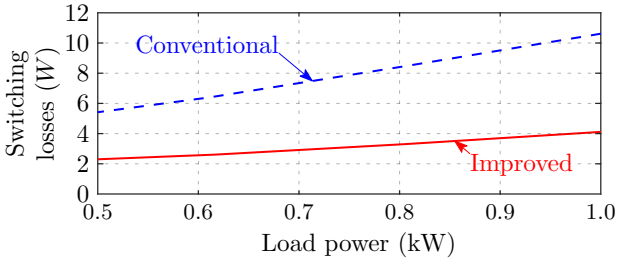

Fig. 7. Simulated total switching losses of the B6-bridge using PLECS for both the conventional and the improved 1P/MB/DSVM schemes. Note that the utilized switch model is C2M0025120D from CREE.

From Table I, it can be seen that the improved 1P/MB/DSVM scheme improves the performance of the three-phase qZSI due to the smaller ST duration of the different switches, which reduces the switching losses for the same operating point.

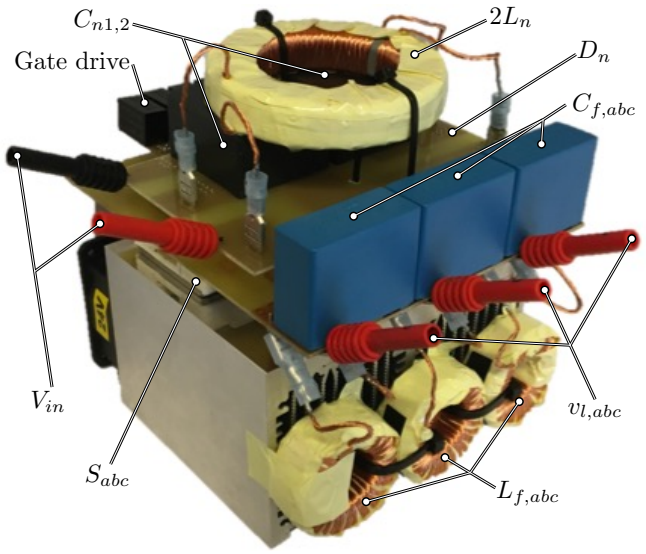

Fig. 8. Experimental prototype of the three-phase qZSI with an output LC filter.

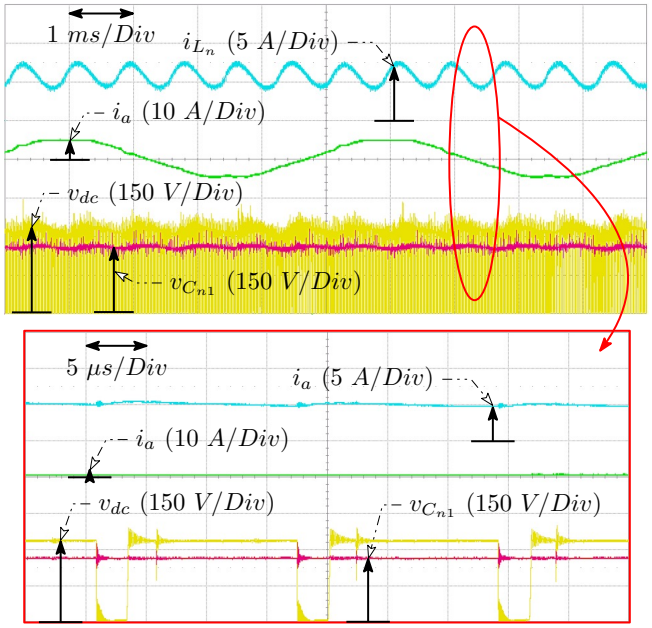

Fig. 9. Obtained experimental results using the proposed modulation scheme using a resistive load of *1 kW*, where the dc-link voltage (v_{inv}), voltage across C_{n1} ($v_{C_{n1}}$), inductor current (i_{L_n}), and load current (i_a) are shown with a zoom for three switching cycles.

IV. Simulation Results

In order to verify the prior analysis and discussions, a *1 kVA* qZSI, whose parameters are listed in Table II, is simulated using PLECS. This qZSI is feeding a resistive load (R_l) through an LC filter as depicted in Fig. 1. Note that M has been set to 0.8564 in order to obtain a fundamental RMS output phase voltage ($V_{\varphi 1}$) of 110 V.

Fig. 6 shows the obtained simulation results using the conventional and the improved 1P-ST/MB/DSVM schemes, in

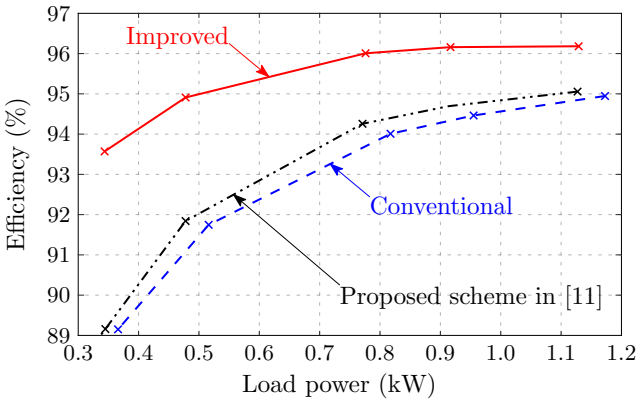

Fig. 10. Measured experimental efficiency of the three-phase qZSI for the conventional and the improved 1P/MB/DSVM schemes, and the introduced modulation scheme in [11].

which the dc-link voltage (v_{dc}), impedance network capacitors voltages ($v_{C_{n1}}$ and $v_{C_{n2}}$), impedance network inductor current (i_{L_n}), and upper and lower switches currents of phase a ($i_{S_{a,u}}$ and $i_{S_{a,l}}$) are shown for each scheme.

These results confirm the prior analysis and verify the functionality of the proposed modulation scheme. Comparing among the different results shown in Fig. 6 for both modulation schemes shows that the improved 1P/MB/DSVM scheme achieves the same operation of the conventional one with an improved performance. Such improved performance is coming out from the simplicity of modulating the different switches and the shorter periods of commutation at the ST current, which is evident from the shown switch currents ($i_{S_{a,u}}$ and $i_{S_{a,l}}$) in Fig. 6. Moreover, it can be seen from the dc-link voltage (v_{inv}) and the inductor current (i_{L_n}) using both schemes, that the effective switching frequency for the conventional 1P/MB/DSVM scheme varies between one to three times the carrier frequency, while for the improved 1P/MB/DSVM scheme it is constant and it is equal to the carrier frequency.

Finally, the switching losses have been calculated using PLECS for both modulation schemes at different load conditions, where the obtained results are shown in Fig. 7. This figure, i.e. Fig. 7, shows that the switching losses under the improved scheme has been significantly reduced due to the shorter periods of commutation at the ST current.

V. Experimental Results

In order to verify the functionality of the improved 1P/MB/DSVM scheme, a three-phase qZSI prototype, which is shown in Fig. 8, is utilized, where the prototype parameters are as listed in Table II.

This prototype has been tested at 1 kW using the improved 1P/MB/DSVM scheme and the obtained results are shown in Fig. 9, in which the dc-link voltage (v_{dc}), voltage across C_{n1} ($v_{C_{n1}}$), inductor current (i_{L_n}), and load current (i_a) are shown as well as a zoom for three switching cycles. These results verify the prior shown simulation results and validates the functionality of the improved 1P/MB/DSVM scheme.

The efficiency of the converter under both the conventional and the improved 1P/MB/DSVM schemes has been measured using a KinetiQ PPA5530 power analyzer, where the obtained measurements are shown in Fig. 10. This figure, i.e. Fig. 10, confirms the merit of improving the converter efficiency due to the shorter periods of commutation at the ST current. In addition, the efficiency of the converter under the introduced modulation scheme in [11] has been measured and showed in Fig. 10, where the improved 1P/MB/DSVM scheme has higher efficiency due to the smaller voltage stresses of the MB and the introduced discontinuity of modulating the switches. Note that this prototype is based on a CCS050M12CM2 SiC power module and a C4D40120D SiC diode from CREE.

VI. Conclusion

In this paper, the conventional single-phase-leg ST-based maximum boost discontinuous space vector modulation (1P/MB/DSVM) scheme has been studied and improved in order to enhance the performance of the three-phase impedance source inverters. Compared to the conventional 1P/MB/DSVM scheme, the improved one has the following merits: simpler implementation due to the utilization of three reference signals, the switches are commutating at the ST current for shorter period during the fundamental period, and thereby is achieving reduced switching losses and improved efficiency as a consequence.

The improved 1P/MB/DSVM scheme has been analyzed and compared to the conventional one, where simulation results using PLECS have been introduced. Moreover, the switching losses have been calculated using PLECS for both schemes, where the improved scheme shows an effective reduction in the switching losses. Finally, experimental results have been introduced in order to verify the reported analysis utilizing a three-phase quasi-Z-source inverter (qZSI) prototype, and these results showed an improved conversion efficiency using the improved 1P/MB/DSVM scheme for the same operating conditions.

References

[1] F. Blaabjerg, K. Ma, and Y. Yang, "Power electronics - the key technology for renewable energy systems," in *Ninth Int. Conf. on Ecological Vehicles and Renewable Energies (EVER)*, Mar. 2014, pp. 1–11.

[2] F. Blaabjerg, Y. Yang, D. Yang, and X. Wang, "Distributed power-generation systems and protection," *Proc. of the IEEE*, vol. 105, no. 7, pp. 1311–1331, July 2017.

[3] A. Abdelhakim, P. Mattavelli, D. Yang, and F. Blaabjerg, "Coupled-inductor-based dc current measurement technique for transformerless grid-tied inverters," *IEEE Trans. on Power Electron.*, vol. 33, no. 1, pp. 18–23, Jan 2018.

[4] A. Abdelhakim, P. Mattavelli, V. Boscaino, and G. Lullo, "Decoupled control scheme of grid-connected split-source inverters," *IEEE Trans. on Ind. Electron.*, vol. 64, no. 8, pp. 6202–6211, Aug 2017.

[5] J. M. Carrasco, L. G. Franquelo, J. T. Bialasiewicz, E. Galvan, R. C. PortilloGuisado, M. A. M. Prats, J. I. Leon, and N. Moreno-Alfonso, "Power-electronic systems for the grid integration of renewable energy sources: A survey," *IEEE Trans. on Ind. Electron.*, vol. 53, no. 4, pp. 1002–1016, June 2006.

[6] F. Z. Peng, "Z-source inverter," *IEEE Trans. on Ind. App.*, vol. 39, no. 2, pp. 504–510, Mar. 2003.

[7] A. Abdelhakim, P. Mattavelli, and G. Spiazzi, "Three-phase split-source inverter (ssi): Analysis and modulation," *IEEE Trans. on Power Electron.*, vol. 31, no. 11, pp. 7451–7461, Nov. 2016.

[8] A. Abdelhakim, P. Davari, F. Blaabjerg, and P. Mattavelli, "Switching loss reduction in the three-phase quasi-z-source inverters utilizing modified space vector modulation strategies," *IEEE Trans. on Power Electron.*, vol. PP, no. 99, pp. 1–1, 2017.

[9] M. Shen, A. Joseph, J. Wang, F. Z. Peng, and D. J. Adams, "Comparison of traditional inverters and z -source inverter for fuel cell vehicles," *IEEE Trans. on Power Electron.*, vol. 22, no. 4, pp. 1453–1463, July 2007.

[10] A. Abdelhakim, P. Mattavelli, P. Davari, and F. Blaabjerg, "Performance evaluation of the single-phase split-source inverter using an alternative dc-ac configuration," *IEEE Trans. on Ind. Electron.*, vol. PP, no. 99, pp. 1–1, 2017.

[11] A. Abdelhakim, P. Davari, F. Blaabjerg, and P. Mattavelli, "An improved modulation strategy for the three-phase z-source inverters (zsis)," in *IEEE Energy Conv. Cong. and Expo. (ECCE)*, Oct 2017, pp. 4237–4243.

[12] M. Zdanowski, D. Peftitsis, S. Piasecki, and J. Rabkowski, "On the design process of a 6-kva quasi-z-inverter employing sic power devices," *IEEE Trans. on Power Electron.*, vol. 31, no. 11, pp. 7499–7508, Nov 2016.

[13] Y. P. Siwakoti, F. Z. Peng, F. Blaabjerg, P. C. Loh, G. E. Town, and S. Yang, "Impedance-source networks for electric power conversion part ii: Review of control and modulation techniques," *IEEE Trans. on Power Electron.*, vol. 30, no. 4, pp. 1887–1906, April 2015.

[14] P. C. Loh, D. M. Vilathgamuwa, Y. S. Lai, G. T. Chua, and Y. Li, "Pulse-width modulation of z-source inverters," *IEEE Trans. on Power Electron.*, vol. 20, no. 6, pp. 1346–1355, Nov. 2005.

[15] F. Z. Peng, M. Shen, and Z. Qian, "Maximum boost control of the z-source inverter," *IEEE Trans. on Power Electron.*, vol. 20, no. 4, pp. 833–838, July 2005.

[16] Y. Zhang, J. Liu, X. Li, X. Ma, S. Zhou, H. Wang, and Y. Liu, "An improved pwm strategy for z-source inverter with maximum boost capability and minimum switching frequency," *IEEE Trans. on Power Electron.*, vol. PP, no. 99, pp. 1–1, 2017.